7. The Complex of Zα with Left-Handed Z-DNA

7.1. Crystallization and Characterization of the Crystals

Initially, small crystals were obtained at 24 °C from a solution containing 600 µM of both Zα protein and the DNA heptamer d(TCGCGCG), 2.5 mM HEPES pH 7.5, 10 mM NaCl, 1 M $(NH_4)_2SO_4$. The solution was equilibrated over 2 M $(NH_4)_2SO_4$. The tetragonal crystals grew rapidly over night, many of them forming clusters. Reduction of the precipitant in the well from 2.0 M to 1.7 M reduced the growth rate. Further, the addition of 10 % glycerol resulted in the growth of large single crystals, suitable for X-ray diffraction experiments. Crystals grew up to (1.0 x 0.3 x 0.3) mm^3 in size.

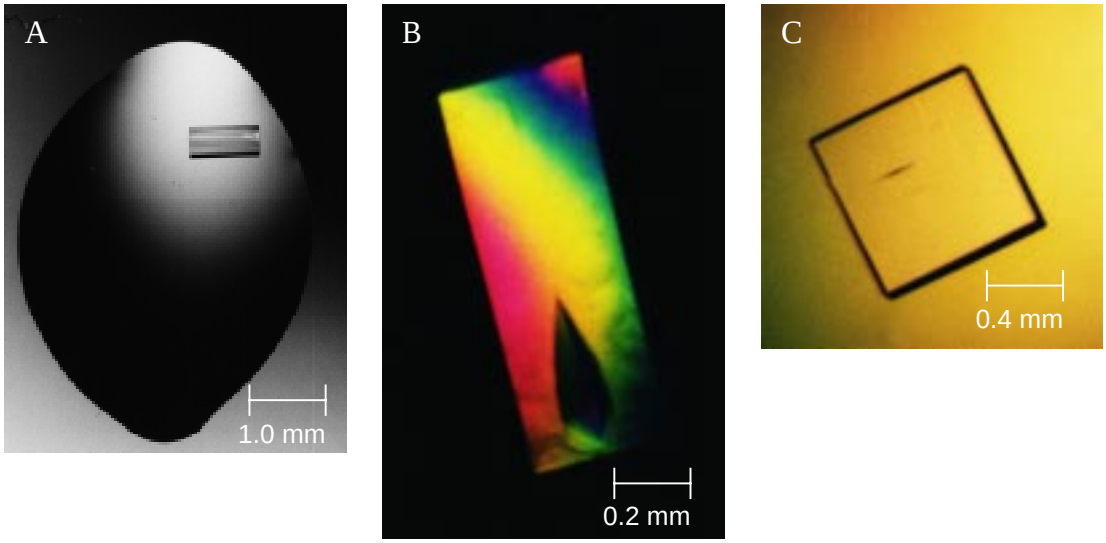

Figure 7.1.1 Crystals of the complex of Zα with the palindromic 6-base-pair deoxynucleotide $d(TCGCGCG)_2$.
The pictures were taken under polarized light. **A**, whole hanging drop setup with one single crystal. **B**, native crystal. **C**, iodo-1 derivative crystal.

The crystals were analyzed to confirm the presence of both protein and DNA. A dissolved crystal produced a Coomassie-stainable protein band on an SDS-PAGE at the expected size for Zα (Figure 7.1.2). DNA was detected spectroscopically: a dissolved crystal resulted in an absorption maximum at 260 nm, characteristic for nucleic acids (data not shown).

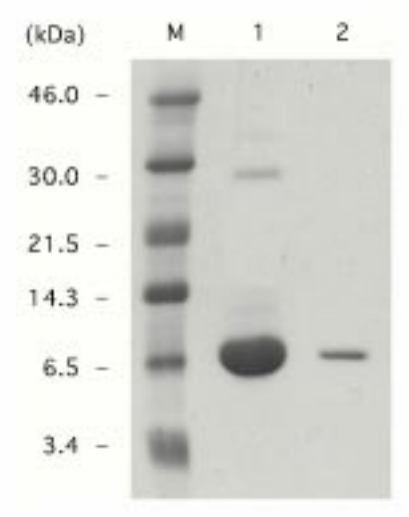

Figure 7.1.2 Gel electrophoretic analysis of the content of a native crystal.
A Coomassie-stained 18 % SDS-PAGE is shown. **Lane M**, molecular weight markers. **Lane 1**, Zα control. **Lane 2**, dissolved crystal.

7.2. Data Collection and Phase Determination

A complete native dataset was collected first (Table 7.2.1). To solve the structure by isomorphous replacement techniques, various strategies were employed. A series of double mutants of Zα were made: 2 serines in the wildtype sequence were pairwise mutated to serines. The mutant proteins were crystallized and soaked with Hg salt solutions in order to obtain suitable derivatives. In a second set of experiments, the DNA substrate was derivatized by substituting 5-iodo-dU for dT or 5-iodo-dC for dC. Crystallization was tried with the purified derivative DNAs. Crystals were obtained with d(^{5I}UCGCGCG, Iodo-1) and with d(TCGCG^{5I}CG, Iodo-6). Derivatizing the DNA substrate proved to be successful: the Iodo-6 derivative allowed for solving the structure with the single isomorphous replacement technique, including

anomalous data (SIRAS). The Iodo-1 derivative was not suitable for phase determination, but these crystals diffracted to a better resolution than the wild-type crystals did. Data collection parameters for all relevant datasets are listed in Table 7.2.1.

	Native	**Iodo-1**	**Iodo-6**
DNA	d(TCGCGCG)	d(^{5I}UCGCGCG)	d(TCGCG^{5I}CG)
Data coverage (Å)	40 – 2.4	20 – 2.1	20 – 2.8
R_{merge} [*] (%)	5.2	7.4	12.0
Number of unique reflections ($I/\sigma I > 0$)	10896	29702	12566
Completeness (%)	99.2	99.9	99.9
Redundancy	6.6	9.8	6.9
R_{iso} [†] (%)	--	--	22.3
R_{ano} (%)	--	--	7.3
R_{Cullis} [¶] (%)	--	--	57.0
Iso. phasing power[§]	--	--	1.34
Anom. phasing power	--	--	1.06
Figure of merit, SIRAS	0.490		
Figure of merit, DM	0.822		
Space group	$P42_12$		
Cell parameters	a = b = 85.9 Å, c = 71.3 Å		
Solvent content	37 %		
Complexes per asymmetric unit	3		

[*] $R_{merge} = \Sigma_h\Sigma_i | I_h - I_{h,i} | / \Sigma_h\Sigma_i I_{h,i}$, where I_h is the mean intensity for the reflection.

[†] $R_{iso} = \Sigma | F_{PH} - F_P | / \Sigma F_P$.

[¶] $R_{Cullis} = \Sigma | | F_{PH} \pm F_P | - F_{H\,calc} | / \Sigma | F_{PH} \pm F_P |$ for centric reflections only.

[§] Phasing power = rms ($F_{H(calc)}$) / rms (phase-integrated lack of closure).

Table 7.2.1 Data collection and SIRAS phasing statistics.

Three iodine positions were located for the Iodo-6 derivative with the program SOLVE (Terwilliger & Berendzen, 1996), using data between 8 and 2.8 Å. Those positions (Table 7.2.2) were used to calculate an initial electron density map. This map, after solvent flattening and phase extension to 2.4 Å, was of astonishing quality (Figure 7.2.3).

	Coordinates (Å)		
Iodine atom	**x**	**y**	**z**
Position 1	19.46	16.80	31.01
Position 2	5.41	13.74	6.75
Position 3	7.26	17.70	17.28

Table 7.2.2 Iodine positions in the Iodo-6 derivative.

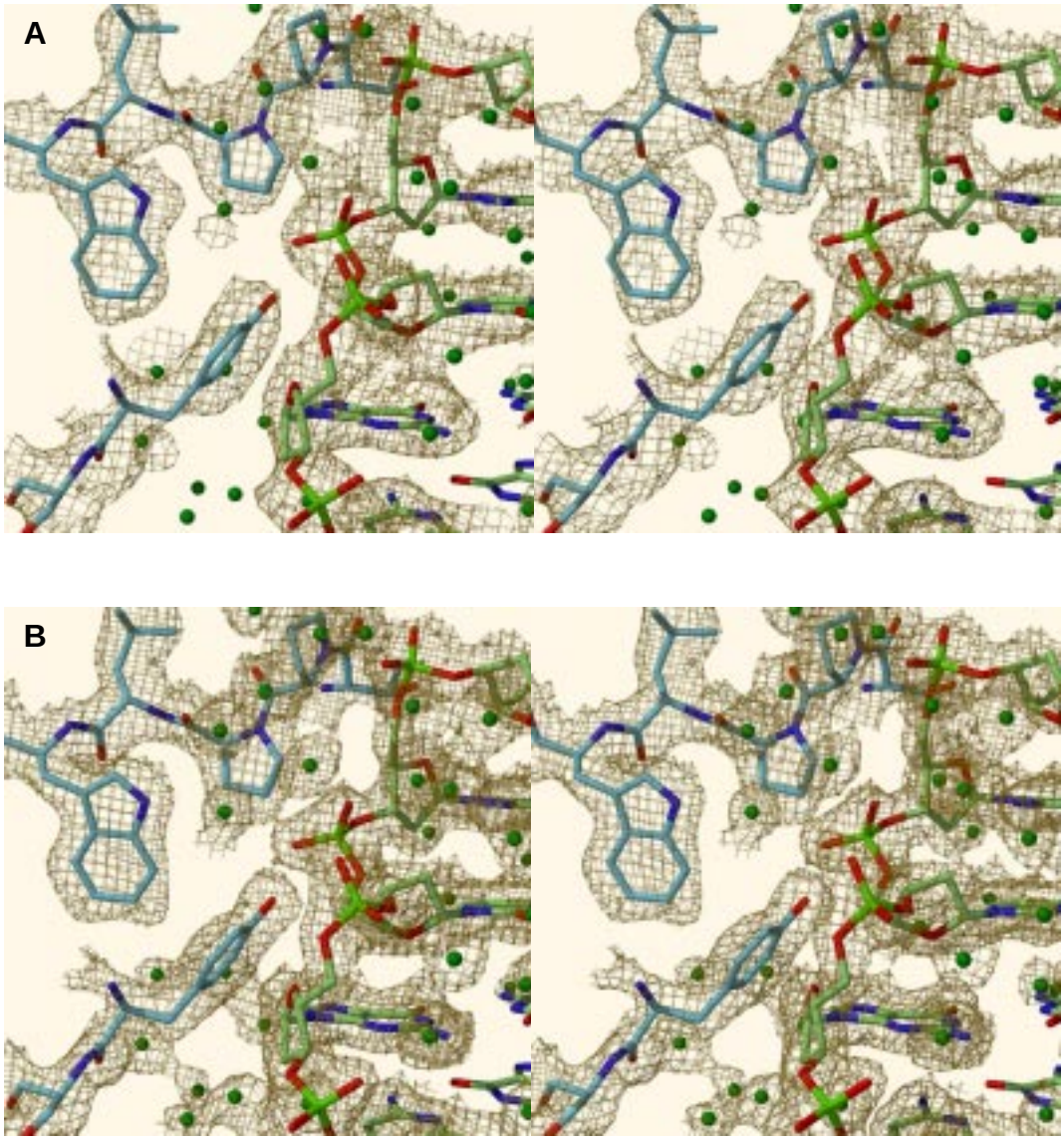

Figure 7.2.3 Electron density maps.
A, stereoview of an experimental map, solvent-flattened and with phases extended to 2.4 Å, showing a segment of the protein-DNA interface. Carbon atoms are light blue in the protein, in the DNA they are light green. Nitrogens are dark blue, oxygens red and phosphors green. Contoured at 1.0 σ. **B**, the identical segment of the protein-DNA interface with the final 2 F_o-F_c-electron density map after refinement. Contoured at 1.0 σ.

7.3. Model Building and Refinement

After solvent flattening with the program DM (Cowtan & Main, 1998), the initial electron density map revealed that the asymmetric unit consisted of three protein-DNA complexes. An initial model was built, comprising three strands

of DNA including backbone and the bases, which are involved in base pairing. The overhanging 5'-dT of the d(TCGCGCG) oligonucleotide was not visible at any stage of the model building process. The main chain of two of the three protein molecules was traced unambiguously. A large number of side chains also was modeled. The third protein molecule in the asymmetric unit was represented significantly more weakly in the initial electron density map. Solvent flattening was repeated, with a lower estimation of the solvent content and the application of an NCS matrix relating the three complexes. (For the first map a DNA duplex and two protein molecules were assumed to form the asymmetric unit. Correspondingly, a solvent content of approx. 50 % was assumed, 13 % higher than the actual content.) Together with phase extension to the resolution limit, 2.4 Å, of the native dataset, this second map largely improved the electron density for the missing protein molecule. Refinement of the entire model was done until R_{free}/R_{cryst} reached a value of 30 %. Then, calculated model phases were combined with the 2.1 Å Iodo-1 dataset. The final model has an R_{cryst} of 22.7 % and an R_{free} of 26.5 %. Model parameters are listed (Table 7.3.1). The main chain torsion angles of Zα show no residues in energetically unfavorable regions (Figure 7.3.2).

Refinement statistics (6-2.1Å)					
R_{cryst} [#] (%)	22.7		**Protein**	**DNA**	**Water**
R_{free} [#] (%)	26.5	Rmsd from ideality:			
Reflections:		Bond lengths (Å)	0.006	0.004	
working set	13772	Bond angles (°)	1.12	0.67	
test set	1531	Average B-factor (Å^2)	32.9	21.9	43.0
N_{atoms}	1898	Rmsd B-factors[*] (Å^2)	3.31	3.19	
N_{waters}	244				

[#] $R_{cryst} = \Sigma | F_P - F_{P\,(calc)} | / \Sigma F_P$, R_{free} is the same as R_{cryst}, but calculated on 10% of data selected evenly over the resolution range and excluded from refinement.

[*] between covalently bonded atoms

Table 7.3.1 Refinement statistics and model parameters.

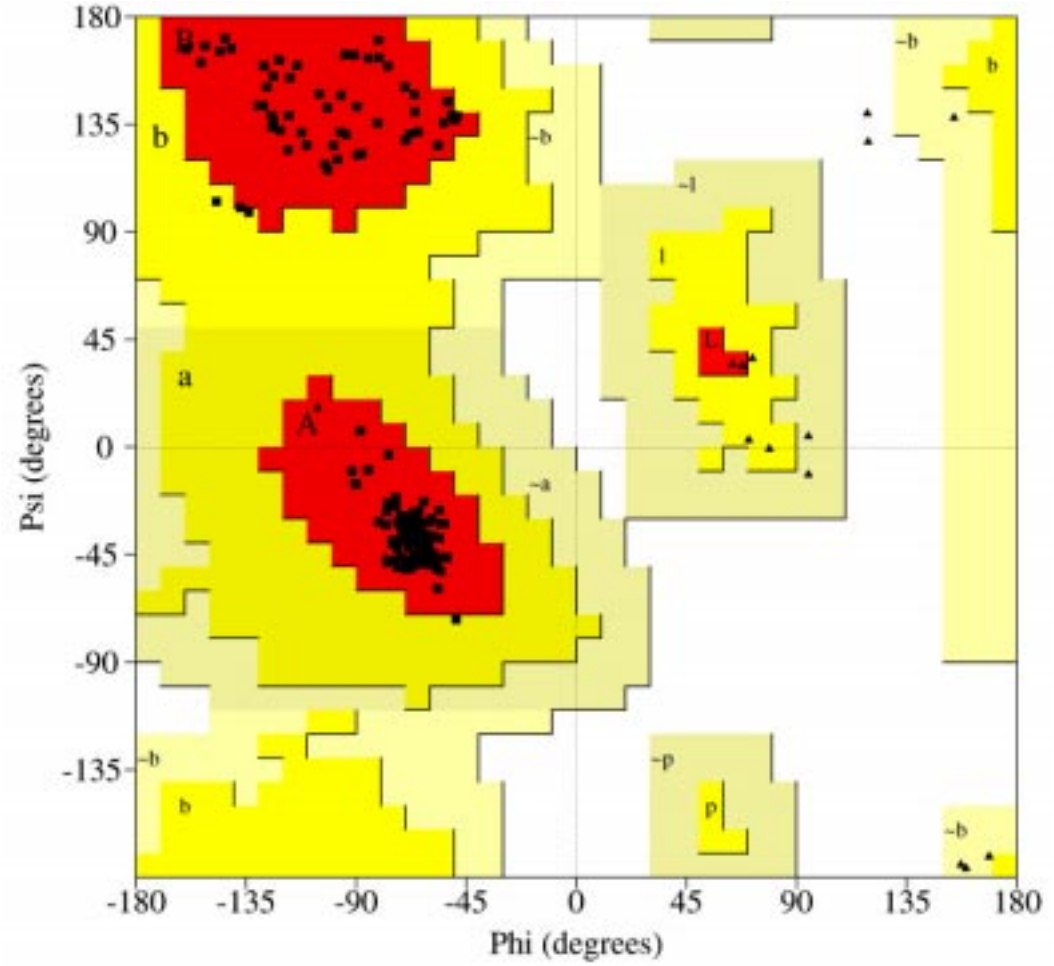

Plot statistics		
Residues in most favored regions (A, B, L)	158	98.1 %
Residues in additional allowed regions (a, b, l, p)	3	1.9 %
Residues in generously allowed regions (-a, -b, -l, -p)	0	0.0 %
Residues in disallowed regions	0	0.0 %
Number of non-glycine and non-proline residues	161	100.0 %
Number of end-residues	6	
Number of glycine residues	18	
Number of proline residues	9	
Total number of residues	194	

Figure 7.3.2 Ramachandran plot.

Non-glycine residues are depicted as filled rectangles; filled triangles represent glycines. All protein residues from the three molecules in the asymmetric unit are shown.

7.4. Overall Structure of the Zα-Z-DNA Complex

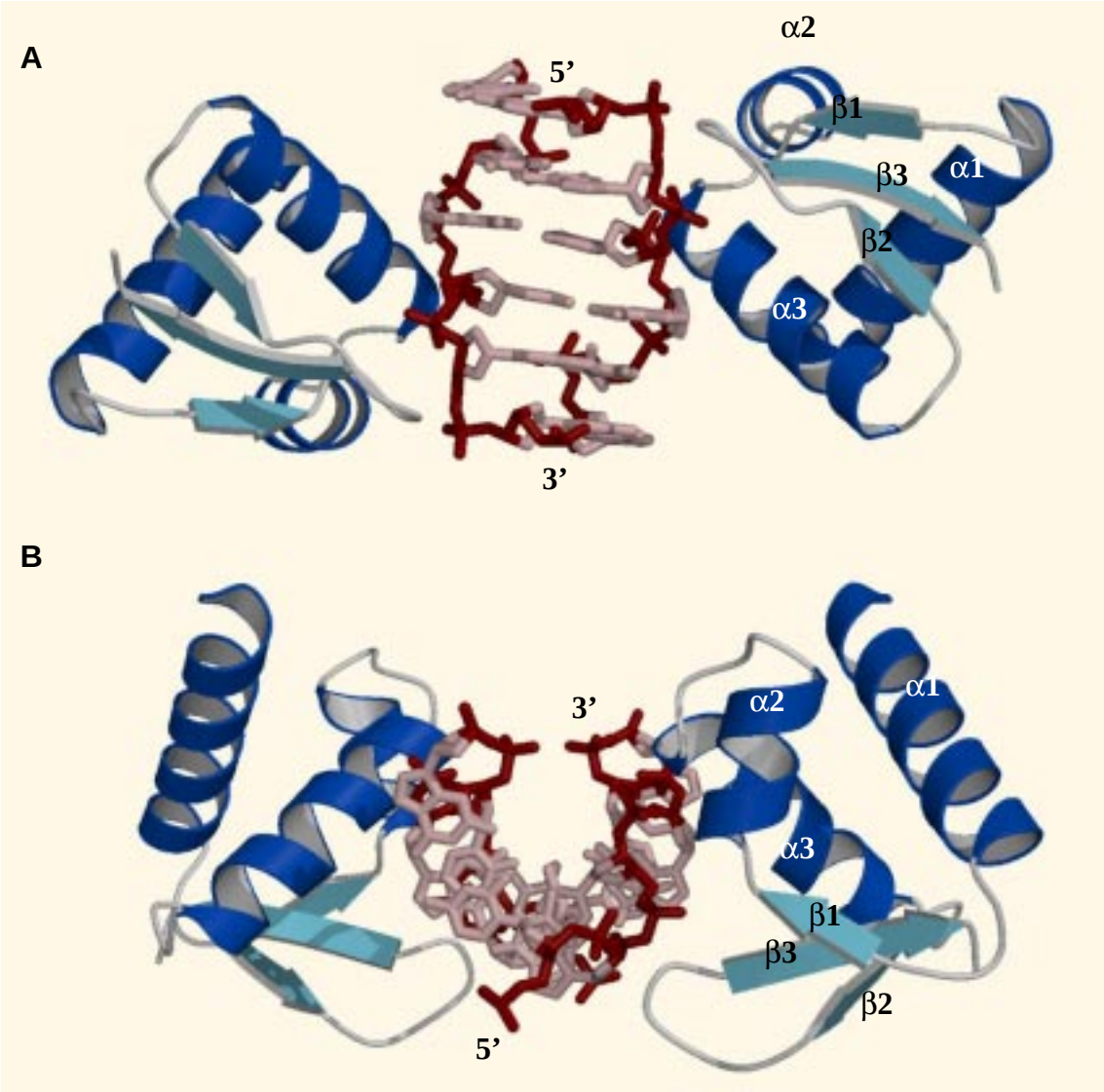

Figure 7.4.1 Overview of the Zα domain bound to left-handed Z-DNA.
Residues 134-198 of two symmetry-related Zα monomers and the 6-bp DNA duplex $d(CGCGCG)_2$ are shown. Labels indicate N- and C-termini of the proteins as well as helices (α1 - α3) and strands (β1 - β3). **A,** view perpendicular to the helical axis of the DNA. **B**, view down the DNA helix, rotated by 90° around the horizontal axis with respect to **A**.

Zα forms a 1:1 complex with a single strand of the 6-base pair DNA duplex (Figure 7.4.1). Two Zα domains, binding to opposite sides of the DNA duplex, are symmetry-related by the twofold axis in the center of the palindromic DNA substrate. The asymmetric unit contains three 1:1 complexes. In one of the two

DNA duplexes the twofold axis coincides with a crystallographic twofold axis; therefore, only one complex is part of the asymmetric unit (a.u.). The second DNA duplex with two protein molecules bound is entirely in the a.u.. In the following chapters, the individual protein molecules in the a.u. are called A, B and C, and the corresponding bound DNA strands D, E and F, respectively. The DNA in the model is built except for the 5'-dT overhang, which appears to be disordered. The protein structure is defined for residues 134-198 in molecule A, 136-198 in B and 134-199 in C. 5 N-terminal (4 of which are vector-encoded) and 11 C-terminal residues of the expressed protein are not unambiguously defined in any of the three domains in the a.u..

The 6-base pair DNA duplex adopts a perfect left-handed Z conformation. Zα is a compact domain and consists of a three-helix bundle (α1 - α3) flanked on one side by a twisted antiparallel β-sheet (β1 - β3). The N-terminal helix, α1 (Ser^{134} – Leu^{150}), is followed by the short strand β1 (Ala^{155} – Thr^{157}), which positions the C-terminal β-hairpin (β2: Leu^{185} – Ala^{188}, β3: Pro^{193} – Ile^{197}) by means of two hydrogen bonds. DNA contacts occur exclusively with helix α3 and the β-hairpin. Zα contacts one strand of DNA on a stretch of 5 consecutive phosphates. The contacts are conformation-specific for Z-DNA: interactions occur mainly with the sugar-phosphate backbone and one additional base contact to a guanine in the syn-conformation, which is conformation- rather than sequence-specific. The two proteins bound to a DNA duplex appear to be independent, since they are not in contact with each other.

7.5. Crystal Packing Interaction

The unit cell consists of 8 asymmetric units, each of which contains three protein-DNA complexes. Thus, the unit cell includes 24 protein-DNA complexes in total (Figure 7.5.1) It has a volume of 526,109 $Å^3$ and a calculated solvent content of 37 %. The solvent content is remarkably low compared to other crystal structures. 244 ordered water molecules were located in this 2.1 Å resolution structure. This relatively high number of ordered solvent molecules might be a result of the low solvent content, since solvent molecules are to a high degree involved in crystal packing interactions (Carugo & Bordo, 1998), and are therefore localized.

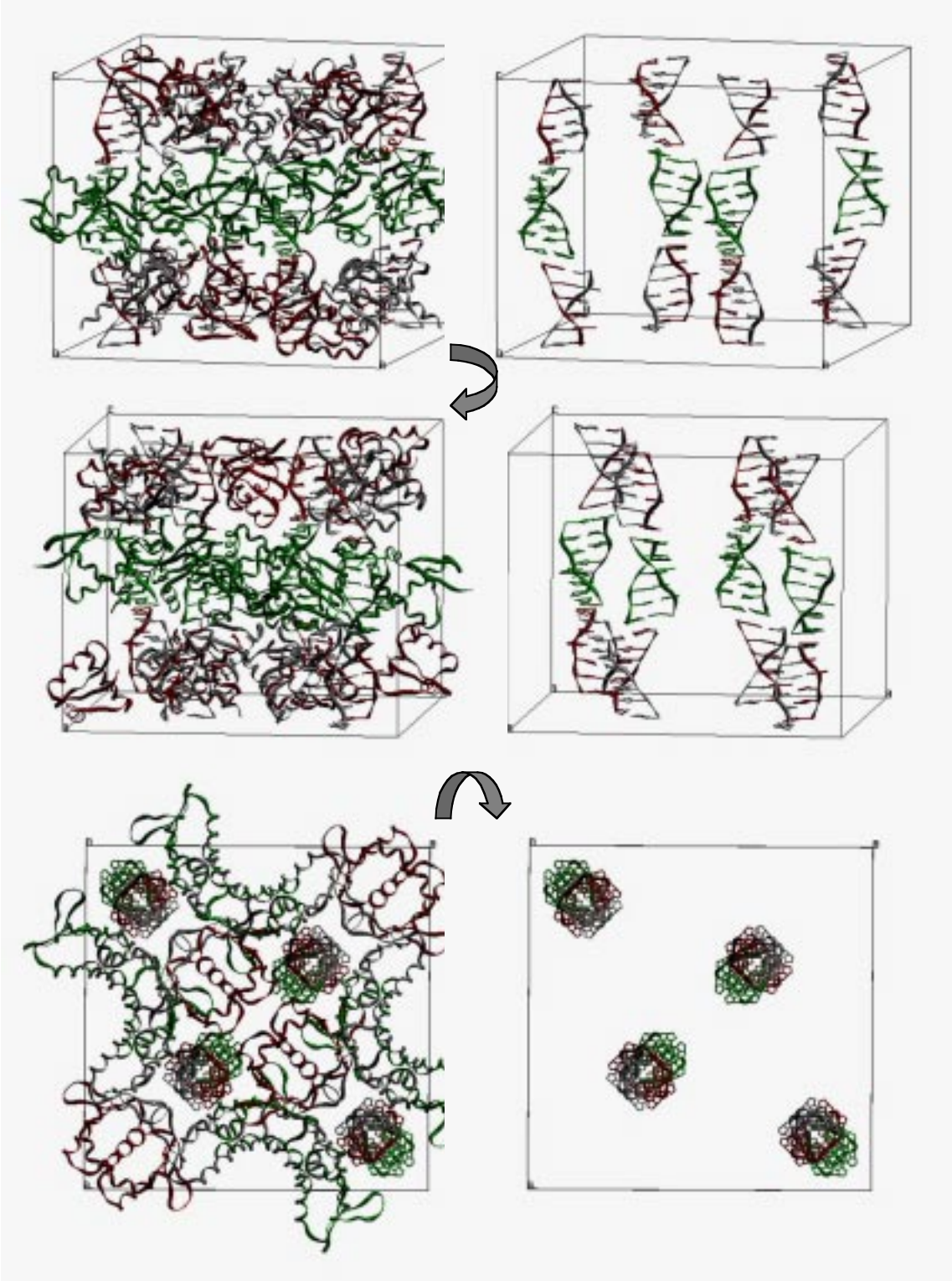

Figure 7.5.1 Crystal packing.

An entire unit cell (space group $P42_12$) is shown in three orientations, which are related by rotations as indicated by the arrows. On the left, all 24 protein–DNA complexes forming the unit cell are displayed. Independent complexes are red, green and grey, respectively. On the right, the unit cell is displayed in the identical orientation but only the DNA is shown.

Packing interactions observed in the crystal lattice involve mainly DNA–DNA and protein–protein interactions between adjacent symmetry-related molecules. The DNA duplexes stack on top of each other and form distorted, pseudo-continuous helices (Figure 7.5.2). Two different stacking interactions are seen in the crystal. At the junction of duplexes on the crystallographic and non-crystallographic axis, respectively, G6 at the 3'-end of the DNA duplex on the crystallographic axis stacks with G6 of the DNA duplex on the non-crystallographic axis. The 5'-ends of both duplexes are not stacked, since the duplexes are laterally displaced with respect to each other. At the other junction, where both adjacent duplexes are on non-crystallographic twofold axes, a quasi-continuous left-handed helix is formed, which is rotated by 90° counterclockwise at the junction. The three protein molecules in the asymmetric unit make extensive interactions with symmetry-related proteins. Zα molecules A and C are involved in such interactions to a much larger extent than molecule B. Molecule B has only some interaction with a symmetry-related molecule B.

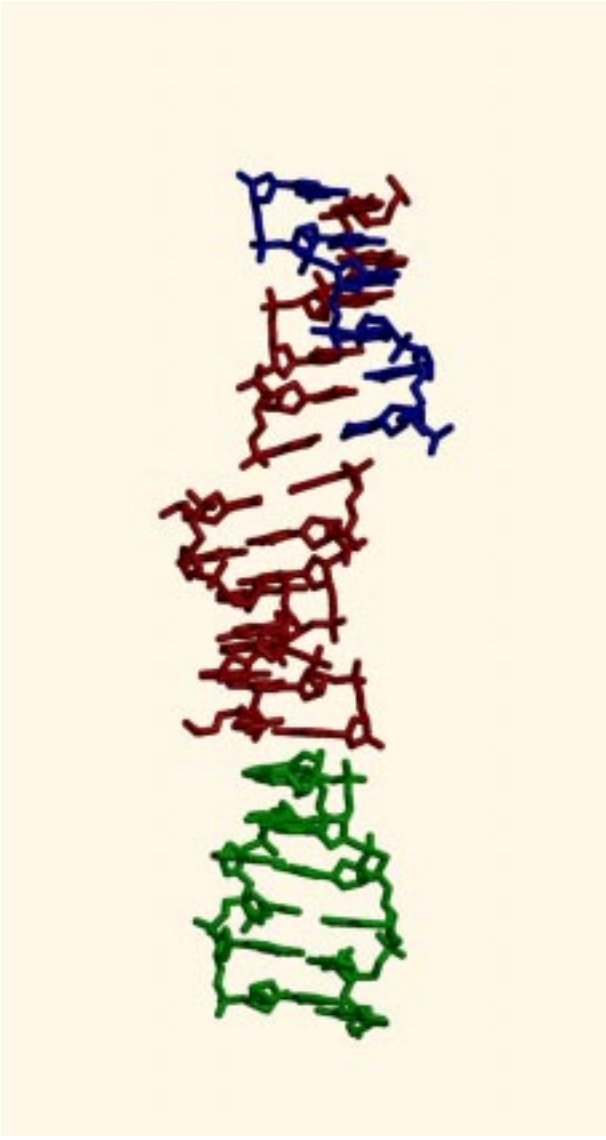

Figure 7.5.2 DNA stacking in the crystal.
DNA strands D, E and F, forming the asymmetric unit, are in red. Strand F', base-pairing with F, is shown in blue. Duplex D'E', which is stacked symmetry-related on duplex DE, is in green. Dupleces DE and D'E' form a pseudo-continuous helix, which is rotationally displaced by 90 degrees. Dupleces DE and FF' are laterally displaced and stack 3' to 3'.

In addition, there is a clash at the N-terminus with the N-terminus of another neighboring molecule B. This apparently distorts the end of helix α1 in B. It might also explain, why the end of helix α1 in molecule B is poorly defined in the electron density map. The comparably small number of crystal packing contacts might be the reason for the poorer quality of the electron density map for molecule B compared to molecules A and C. Molecule B has a higher flexibility and so the average electron density at a given position is lower than in the more rigidly coordinated molecules A and C. This is also reflected in the average temperature factor, which is higher for molecule B (46.4 $Å^2$) than for A (29.2 $Å^2$) or C (27.4 $Å^2$), respectively.

Molecule A has lattice interactions with symmetry-related molecules A and C. Helix α1 and turn 1 are involved in numerous direct, ionic and water-mediated contacts with the neighboring molecules. Molecule C is also strongly contacted through packing interactions. Besides some interactions with two molecules A, there are extensive contacts to two molecules C, which are related by the fourfold axis of the space group (Table 7.5.3).

Protein	Contact with symmetry-related molecule	Contact area (Å)
A	A1	363
	A2	363
	C3	191
	C4	245
	total	**1165**
B	B1	18
	B2	190
	total	**208**
C	A4	245
	A5	191
	C1	381
	C2	381
	total	**1198**

Table 7.5.3 Crystal packing contacts of Zα molecules.

7.6. The Zα Domain

The compact Zα domain can be described as a roughly tetrahedral entity with dimensions of 25 x 31 x 32 $Å^3$ (Figure 7.4.1). The solvent-exposed parts of the three-helix bundle formed by α1 - α3 constitute three planes of the tetrahedron; the exposed side of the antiparallel β-sheet is the fourth plane. Superimposing the three protein monomers in the asymmetric unit reveals differences in the peptide backbone trace in two areas (Figure 7.9.1). Strongest are the deviations in the first two turns of helix α1. This is most likely due to the distortion observed in molecule B, where a clash with a symmetry-related molecule is observed (see chapter 7.5). The loop region following helix α1 is the second area, where backbone deviations between molecules A, B and C are observed. The position of these loop residues is largely affected by crystal packing forces. Higher temperature factors for these loop residues, compared to rest of the molecule, indicate that they have a higher apparent flexibility. Figure 7.6.1 shows that residues in molecule B have higher B-factors than in A and C, reflecting more flexibility.

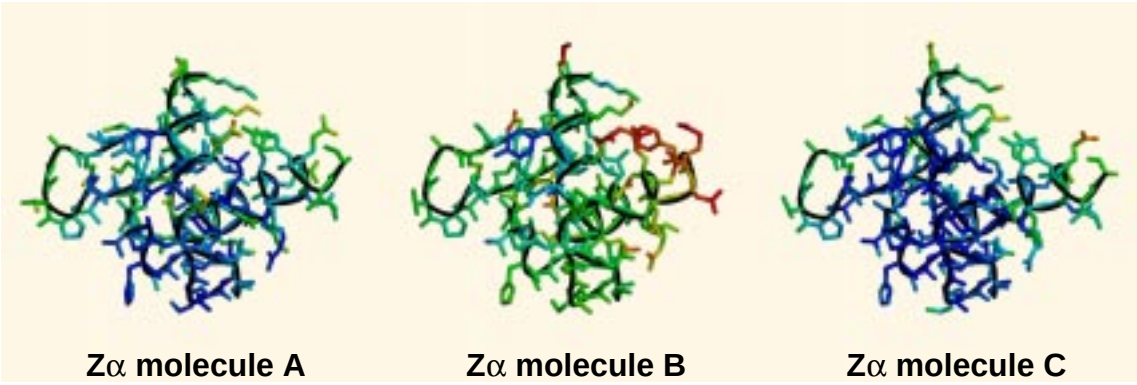

Figure 7.6.1 Temperature factor comparison.
Models of the three independent Zα monomers A, B and C in the crystal in identical orientation. Atoms are gradient-colored according to their temperature factors: red for highest, blue for lowest values. The Cα-backbone trace is shown in black. Residues in molecule B have higher average B-factors than identical residues in molecules A or C.

Within the Zα domain, B-factors are lowest for helices α2 and α3, as well as for residues buried in the core of the protein. Residues from all three helices and strand β3 form a hydrophobic core (Figure 7.6.2). The surface lacks significant

hydrophobic areas, but it is highly charged. The charge distribution is asymmetrical, with positive charges concentrated on the side, which forms the protein-DNA interface (see Figure 7.8.3).

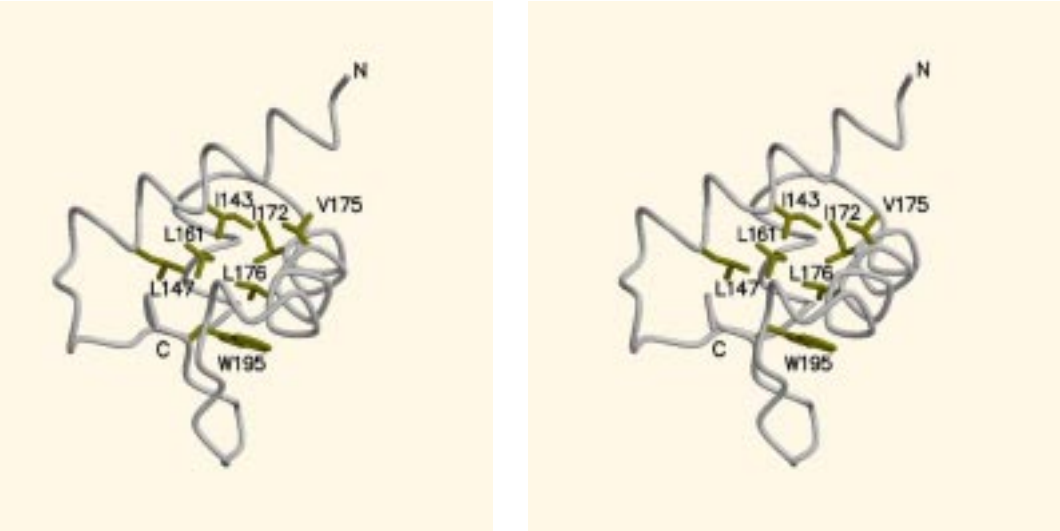

Figure 7.6.2 Hydrophobic core of Zα.
Stereoview of the Zα domain with residues forming the hydrophobic core shown in yellow. The white coil represents the Cα-backbone trace of the protein.

7.7. The Left-Handed Z-DNA

The palindromic 6-base pair $d(CGCGCG)_2$ DNA duplex adopts an undistorted Z conformation. Guanines are in the syn-conformation and have C3'-endo sugar puckers, characteristic of Z-DNA. The structure is very similar to the originally described Z-DNA structure of a $d(CGCGCG)_2$ hexanucleotide (Wang *et al.*, 1979) (Figure 7.7.1). A superposition with this structure reveals an rms deviation of 0.82 Å for the DNA duplex formed by strands D and E, and 0.83 Å for the DNA duplex made by strand F and its symmetrymate F'. These rms deviations are remarkably low considering the fact that the mean coordinate error of the Zα-Z-DNA complex is 0.30 Å (calculated with SfCheck; from CCP4, 1994).

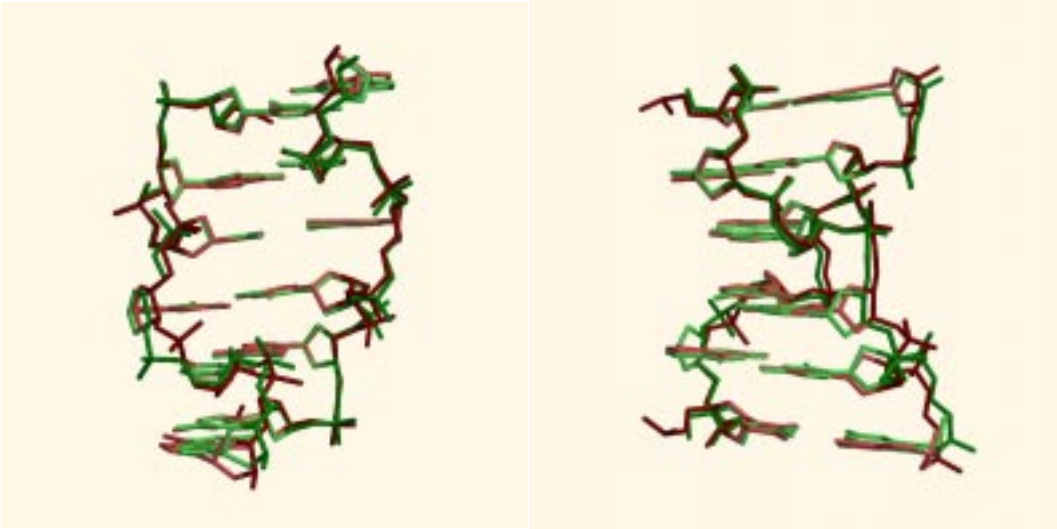

Figure 7.7.1 DNA superposition.
The duplex DE of this crystal structure is shown in red. In green, the pure DNA crystal structure of the left-handed DNA duplex $d(CGCGCG)_2$, (Wang *et al.*, 1979; PDB Code 1DCG).
Both structures superimpose with an rms deviation of only 0.82 Å. The view on the right is rotated around the helical axis by 90 degrees with respect to the view on the left.

The structure of the DNA duplex $d(CGCGCG)_2$ has been determined crystallographically under various conditions (different additives in the solution used for crystallization, data collection under ambient or cryo conditions). Two alternate locations of the phosphate group at the G4pC5 step have been observed, called Z_I and Z_{II} (Wang *et al.*, 1981; Gessner *et al.*, 1989), as a result of those varying conditions. In the complex of $d(CGCGCCG)_2$ with Zα, all phosphate groups are in the Z_I conformation.

7.8. Protein-DNA Contacts

The contact between Zα and the DNA strand consists of a single continuous recognition surface (Fig. 7.8.1). This surface, which is complementary to the DNA in terms of shape and electrostatic nature, consists of residues from helix α3 and the C-terminal β-hairpin. All the polar and ionic interactions in the complex are with the sugar-phosphate backbone and not the bases. A stretch of 5 consecutive phosphates is contacted by the protein. Ionic interactions involve Lys^{169}, Lys^{170} and Arg^{174} in helix α3 and non-esterified oxygens at the C3pG4 and C4pG5 steps. Polar contacts with the DNA are made with Asn^{173} and Tyr^{177} in helix α3 as well as Thr^{191} in the β-hairpin loop. In addition, water-mediated backbone contacts are observed. Lys^{169}, Asn^{173}, and Trp^{195} coordinate two ordered water molecules embedded within the protein-DNA interface in all three independent complexes. These waters are completely shielded from the bulk solvent. Further, Thr^{191} and Arg^{174} also bind to the furanose oxygens of G2 and G6, respectively. This ensemble of residues forms an extensive network of hydrogen bonds; four of the five consecutive phosphate groups are grasped by at least two hydrogen bond donors (Figures 7.8.1, 7.8.2).

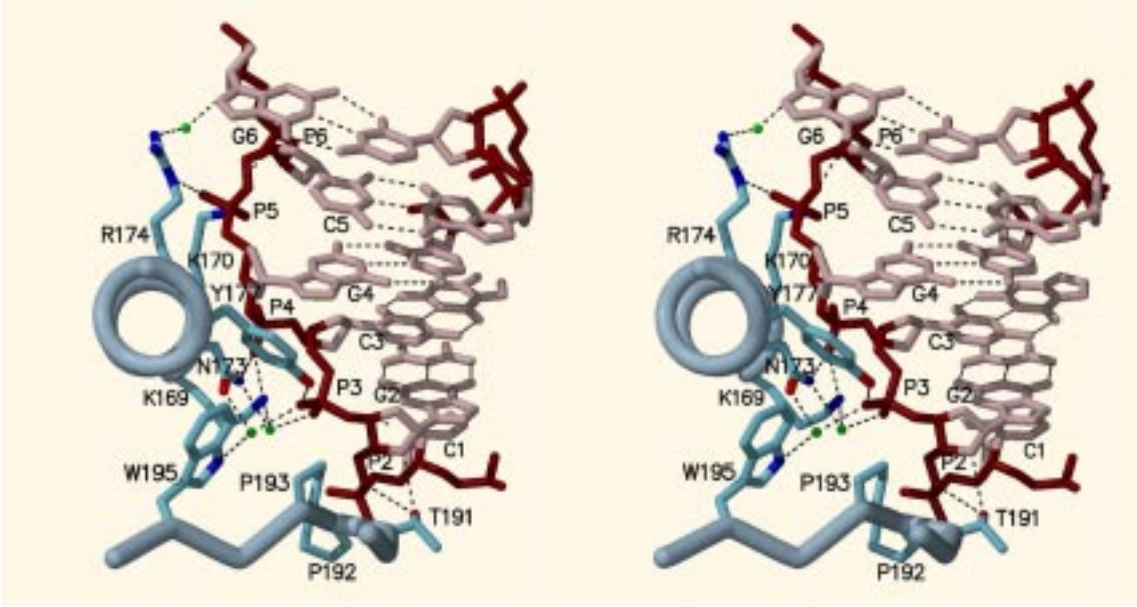

Figure 7.8.1 Zα-Z-DNA interface.

The stereo view (down the axis of the recognition helix α3) shows the entire region of the DNA recognized by Zα. Five consecutive backbone phosphates of the DNA are contacted by an extensive hydrogen bonding network. Protein side chains in direct or water-mediated contact with the DNA are labeled. Water molecules are in green. Tyr^{177} is involved in the only base contact seen in the complex, and is in van der Waals contact with the exposed C8 of the purine base G4, characteristic of Z-DNA.

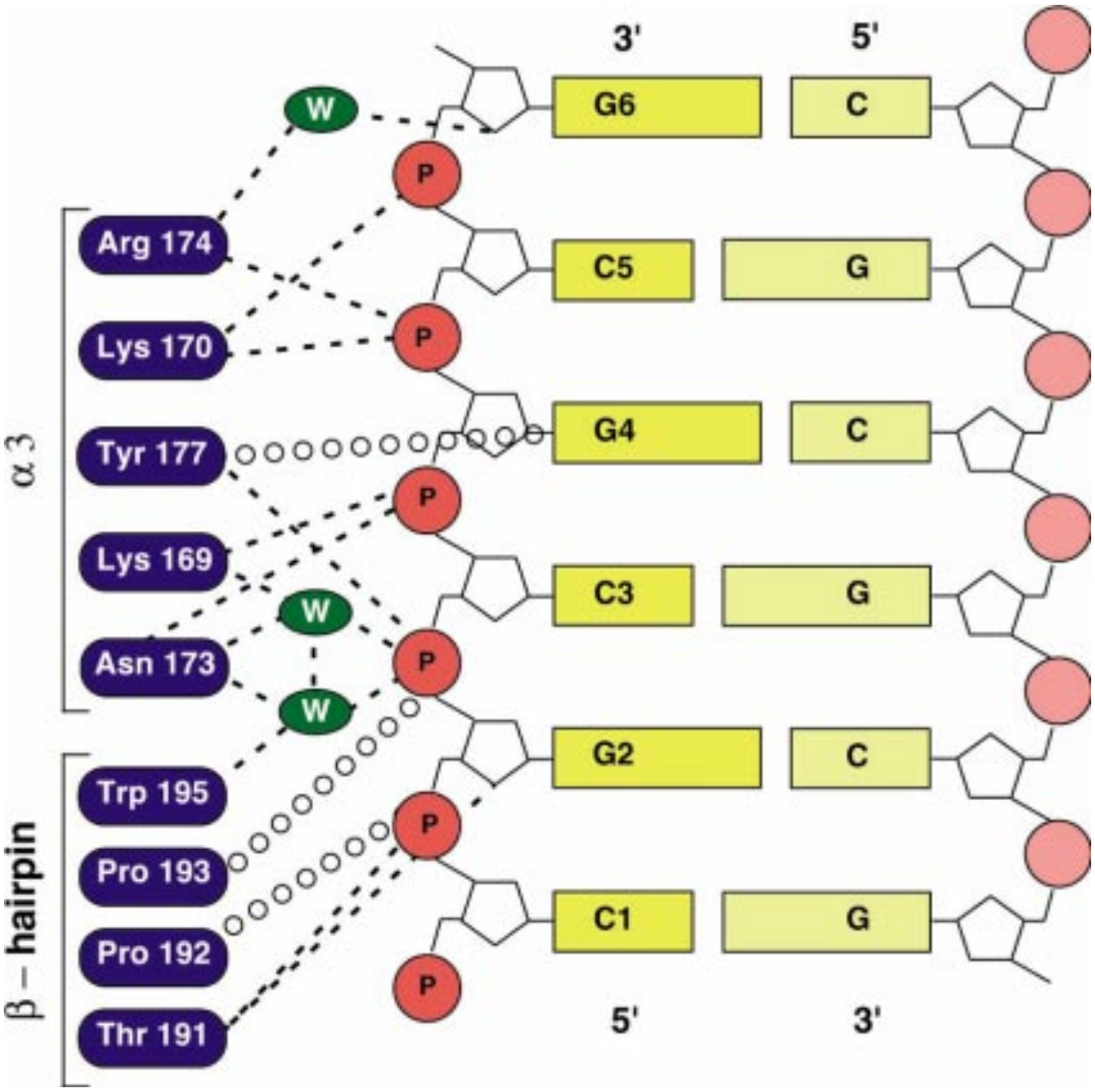

Figure 7.8.2 Schematic representation of Zα-Z-DNA contacts.

Diagram showing the protein residues involved in DNA interactions. All contacts are between the protein and one strand of the DNA duplex. Hydrogen bonds are indicated by dashed lines, van der Waals contacts by open circles. Three water molecules in key positions within the protein-DNA interface are drawn as green ovals.

In concert with these ionic and polar interactions, the crystal structure reveals a striking complementarity in the van der Waals surfaces of the protein and the DNA (Figure 7.8.3).

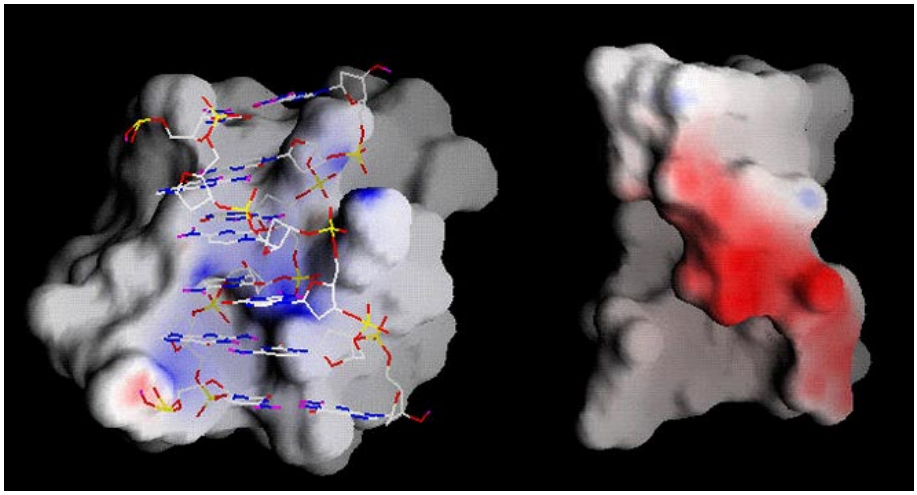

Figure 7.8.3 Electrostatic surface reresentation of the Zα-Z-DNA interface.

Peptide backbone atoms of helix α3 (Lys^{170}, Arg^{174}) contact the ribose of G4. The face of the aromatic ring of Tyr^{177} makes a close van der Waals contact with the exposed C8 of guanine 4. This interaction is only possible if this base is in *syn* conformation and is therefore specific for Z-DNA. The phenolic side chain of Tyr^{177} is almost perpendicular to the G4 base. Further, the aromatic ring of Trp^{195} is perpendicular to the Tyr^{177} ring from the other side, and buttresses it from within the protein core. Similar systems of mutually perpendicular aromatic rings in an edge-to-face orientation have been shown to stabilize other protein-ligand interactions (Burley & Petsko, 1988). In Zα, Trp^{195}, positioned precisely within the hydrophobic core, maintains two important indirect DNA contacts, via Tyr^{177} and via a water to the backbone. This central role of Trp^{195} explains the detrimental effect of W195A and W195Y mutations on both protein stability and DNA binding, as well as the tryptophan fluorescence quenching observed as a result of Z-DNA binding (Berger *et al.*, 1998; Schade *et al.*, 1999). Pro^{192} and Pro^{193} in the C-terminal β-hairpin form another important van der Waals interaction with the DNA. The pyrrolidine rings of both residues pack against the sugar-phosphate backbone from phosphate 2 to phosphate 3. In

contrast to the predominant trans peptide linkage, Pro[192] forms a *cis* peptide bond, thereby positioning the β-hairpin loop against the DNA surface (Figure 7.8.4).

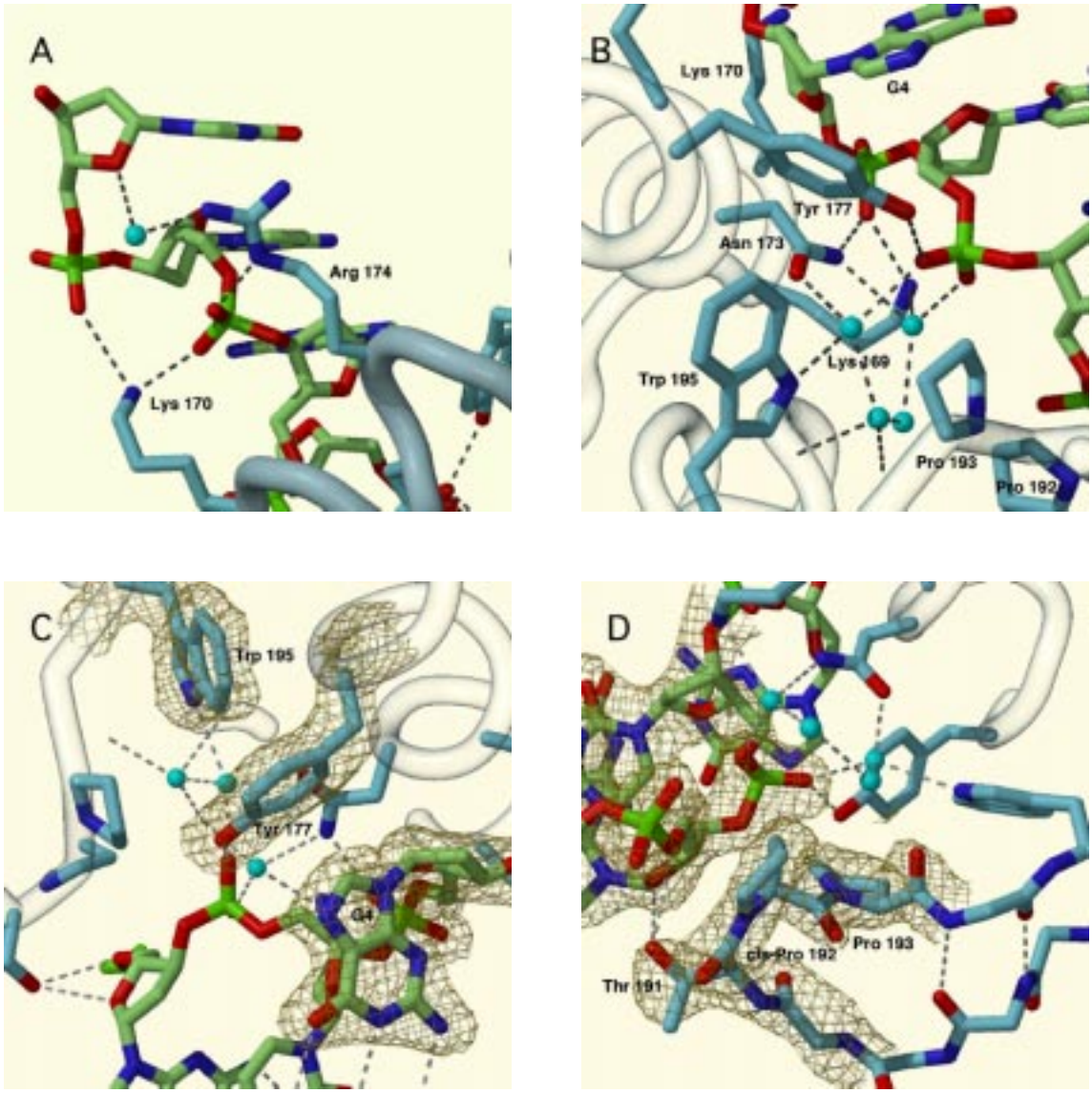

Figure 7.8.4 Close-ups of the Zα-Z-DNA interface.
A, ionic and water-mediated DNA backbone contacts via Lys[170] and Arg[174]. **B**, core region of the Zα-Z-DNA interface. Buried water molecules are integrated in the complex structure through numerous hydrogen bonds. **C**, the only base contact of the interface. The G4 base, Tyr[177] and Trp[195] are mutually perpendicular in edge-to-face orientation. This interaction is possible only with a nucleoside in the syn conformation, characteristic of Z-DNA. **D**, Thr[191], cis-Pro[192] and Pro[193] form a van der Waals surface complementary to the characteristic 'zig-zag' backbone of the Z-DNA substrate.

7.9. Comparison of the Three Independent Zα-DNA Complexes in the Asymmetric Unit

The three independent Zα-DNA complexes in the asymmetric unit were refined completely independently, i.e., without using non-crystallographic symmetry restraints. In general, this method prolongs the refinement procedure, but reduces the danger of model bias. After the refinement, all three complexes were superimposed (Fig. 7.9.1). Rms deviations were calculated (Table 7.9.2). The three complexes are remarkably similar in their structure. The protein-DNA interface is almost invariant. Deviations are seen for Arg^{174} and Thr^{191}. The electron density for the Arg^{174} side chain is not as well defined as it is for other side chains in the complex. Since it is partially solvent-exposed, it might exhibit some flexibility. An R174A mutant was shown to be capable of binding to Z-DNA as well, implying that its interaction with Z-DNA is not crucial (Schade *et al.*, 1999). The Thr^{191} position is slightly different in the three complexes, although in all cases the hydrogen bond with the furanose oxygen of G2 is maintained. Parts of the protein not involved in DNA contacts vary only marginally, as discussed in section 7.6. The DNA strands superimpose almost exactly. Slight variations occur in the position of the terminal bases, possibly due to packing forces. The close similarity between the three complexes also includes 20 water molecules at identical positions. Among them are the water molecules involved in DNA contacts in the center of the protein-DNA interface.

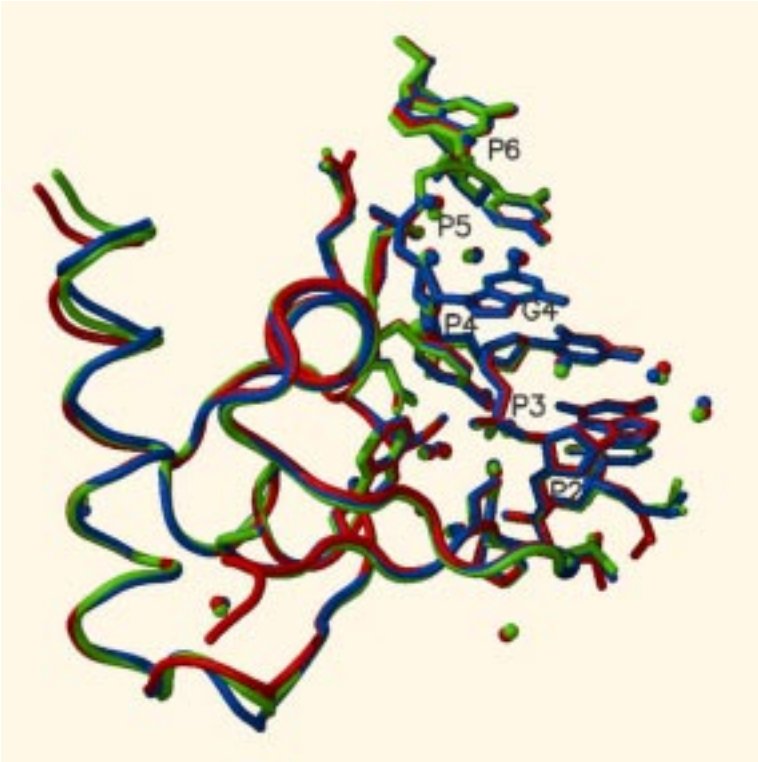

Figure 7.9.1 Superposition of the three independent Zα-Z-DNA complexes in the asymmetric unit.

Complex of Zα molecule A with DNA strand D is in green, complex BE in blue and complex CF in red. Water molecules, observed at identical positions in all three complexes, are shown in matching colors.

		rms deviation (Å)		
		all atoms	Cα-trace	Cα-trace +DNA
Complex	BE on AD	0.8784		0.3236
	CF on AD	0.7886		0.5330
	CF on BE	0.9986		0.5825
Protein	B on A	0.8062	0.3397	
	C on A	0.7521	0.4674	
	C on B	0.9383	0.6194	
DNA	E on D	0.2558		
	F on D	0.5457		
	F on E	0.5372		

Table 7.9.2 Rms deviations between the three independent crystallographic models.

7.10. Structural Classification of the Zα Domain

It has been proposed from secondary structure predictions and low resolution NMR studies that Zα might belong to the class of helix-turn-helix (HTH) proteins (Herbert *et al.*, 1997; Schade *et al.*, 1999). This crystal structure proves this assumption correct. A comparison of Zα with protein coordinates taken from the PDB, using the program Dali (Holm & Sander, 1995), is shown (Table 7.10.1).

Protein	PDB code	Σ Cα	Rms dev. (Å)
Metallothionein repressor SmtB	1SMT	44	0.7853
Restriction endonuclease FokI D1 domain	2FOK	38	1.183
Biotin operon repressor BirA	1BIA	37	1.196
Transcriptional repressor LexA	1LEA	45	1.156
Histone H5	1HST	39	1.282
Transcription factor E2F-4	1CF7	42	1.306
Catabolite gene activator CAP	2CGP	43	0.9423

Table 7.10.1 Rms deviations between Zα and related helix-turn-helix proteins.
The proteins were found with the program Dali (Holm & Sander, 1995). The structures were compared with Superimpose (M.A. Rould, personal communication) and rms deviations calculated for Cα-positions at structurally equivalent positions (i.e., Cα-positions are less than 1.5 Å apart between the two compared structures).

Rms deviations of structurally equivalent Cα positions show that the similarity is most striking between Zα and the bacterial metallothionein repressor SmtB (Cook *et al.*, 1998), but another group of HTH proteins is also closely related. The HTH protein family has been subdivided into classes of similar structure (Wintjens & Rooman, 1996). Among those classes, Zα belongs to the HTH proteins with α/β topology. In common, they share a core fold containing a three-helix bundle closed by an antiparallel three- or four-stranded β-sheet. A structural comparison of Zα with related proteins is illustrated (Fig. 7.10.2).

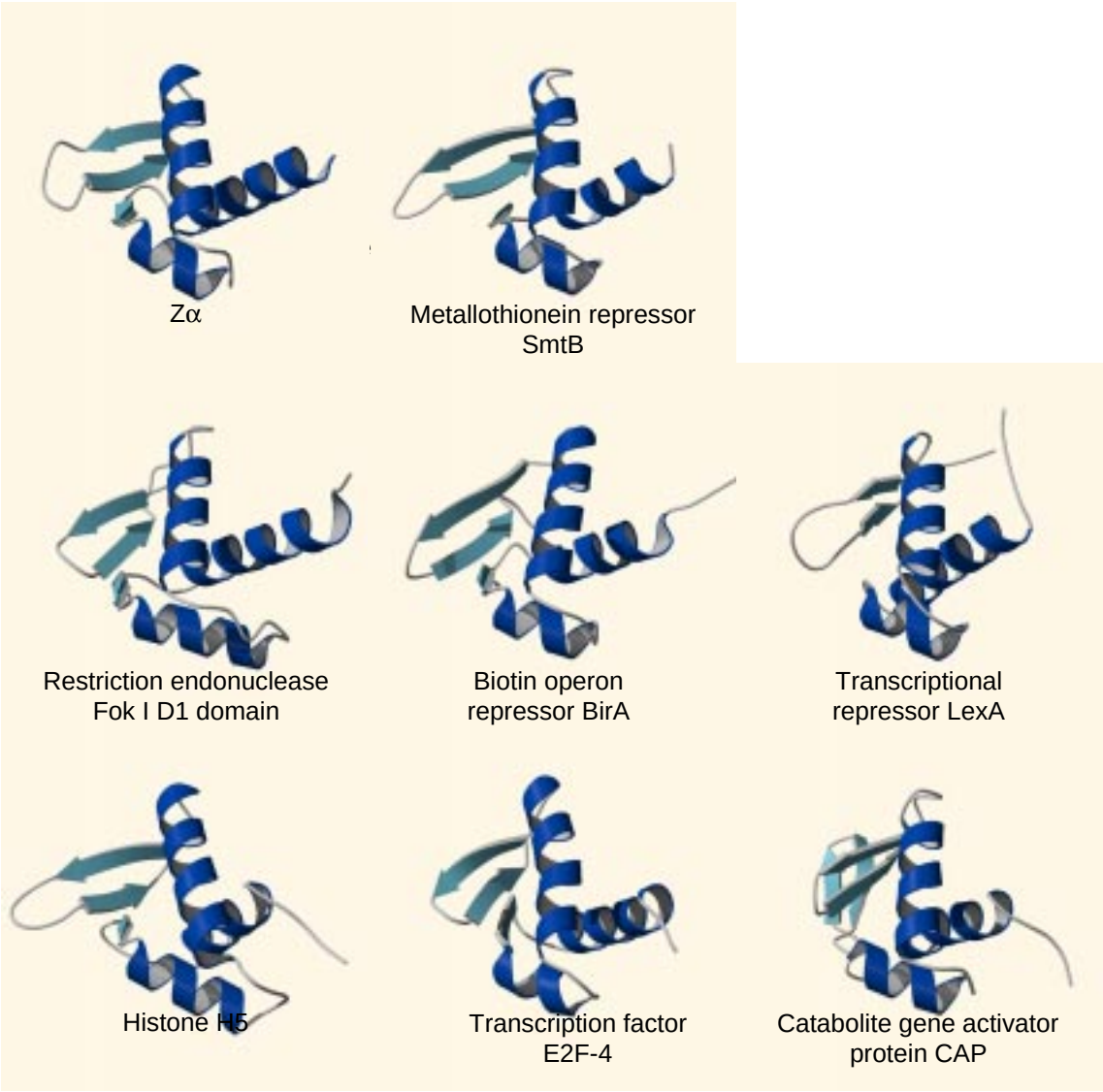

Figure 7.10.2 Structural comparison of related HTH proteins with α/β topology.